https://doi.org/10.7840/kics.2024.49.6.801

Quadrature Amplitude Modulation with Circular Boundary

Minuk Seong◆, Sung-Joon Park°

ABSTRACT

In modern digital communication systems, square quadrature amplitude modulation with a high modulation order is widely used to increase spectral efficiency. In this paper, we propose a new quadrature amplitude modulation with a square lattice and a circular boundary and investigate its power gain and peak-to-average power ratio using heuristic and analytic methods. The results show that the proposed modulation provides a power gain of 0.2003 dB and a 33% reduction in the peak-to-average power ratio when compared with the conventional square quadrature amplitude modulation.

Key Words : QAM, signal constellation, bits-to-symbol mapping, PAPR, power gain

Ⅰ. Introduction

High-order modulation transmitting multiple bits per symbol is widespread in digital communication systems because it ensures fast data transfer. Combined amplitude and phase modulation schemes have been studied to find an efficient constellation in a two-dimensional signal space[1-3]. Foschini et al. used a gradient search algorithm in an attempt to find an optimal constellation[4]. The constellation designed on a triangular lattice has been investigated in a previous study[5]. Design and analysis of other high-order modulations can be found in the literature [6-8]. Among all these constellations that enhance spectral efficiency, square quadrature amplitude modulation(SQAM)[3] is the most common constellation. It is exclusively used in various applications owing to its reasonable performance and simple detection.

In this study, we focus on the modulation schemes with a square lattice, where signal points are located at the intersection of the lattice. From the motivation to determine the best square-lattice constellation in terms of maximizing the efficiency of energy use, a quadrature amplitude modulation with a circular boundary is naturally devised. Symbol selection and bit mapping methods are investigated to complete the proposed constellation. Further, the power gain and the peak-to-average power ratio (PAPR) of the proposed modulation are found by heuristic and analytic methods and are compared with those of SQAM.

Ⅱ. Signal constellation of circular QAM

2.1 Symbol Selection

Fig. 1 shows the signal constellation of the conventional SQAM for the M-ary signal sets (M = 16, 64, 256, and 1024). The parameter d denotes half the minimum Euclidean distance between adjacent signal points. In general, SQAM is defined over M $= 2^{2M}$, where m is an integer, and thus it has a square-shaped boundary. For an arbitrary signal point s_i, the symbol energy of s_i is defined as

$$\|s_i\|^2 = s_{i,I}^2 + s_{i,Q}^2 \quad (1)$$

where $s_{i,I}$ and $s_{i,Q}$ represent the real and imaginary

※ This work was supported by the NRF grant funded by MSIT (2020R1F1A1048594).
◆ First Author : Gangneung-Wonju National University Department of Electronic Engineering, semiwo0713@gwnu.ac.kr, 학생회원
° Corresponding Author : Gangneung-Wonju National University Department of Electronic Engineering, psj@gwnu.ac.kr, 정회원
논문번호 : 202401-013-B-RU, Received January 10, 2024; Revised February 8, 2024; Accepted February 8, 2024

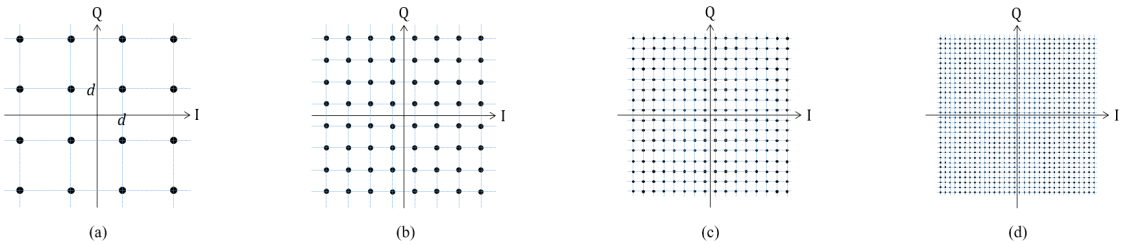

Fig. 1. SQAM constellation: (a) 16-ary, (b) 64-ary, (c) 256-ary, (d) 1024-ary

values of s_i, respectively. Owing to the regular structure of SQAM, the average symbol energy of SQAM, E_s, can be easily calculated as

$$E_s = \frac{1}{M}\sum_{i=1}^{M}\|s_i\|^2 = \frac{2}{3}(M-1)d^2 \quad (2)$$

Meanwhile, the efficiency of SQAM associated with energy use is degraded by signal points near the edge of the constellation. Since the constellation having a circular envelope would be more efficient, we propose a new constellation with a square lattice that reduces the average energy per symbol. The following procedure is applied for the acquisition of this constellation:

[Step 1] Locate the first signal point at (d, d).

[Step 2] Among the remaining candidates placed at the intersection of the square lattice, choose the point with the minimum symbol energy as the second signal point. If multiple points have the same minimum energy, select one randomly.

[Step 3] Except for the signal points that are chosen already, repeat the process given in Step 2 until M signal points are all selected.

Fig. 2 illustrates the constellation obtained through the above process for M = 16, 64, 256, and 1024. In the case of the 16-ary signal set, there is no difference between the conventional and proposed constellations. However, as M increases, the boundary of the proposed constellation approaches quickly the shape of the circle. This is because the signal points are selected based on the strategy of minimum energy. For this reason, hereafter, we will call the constellation circular SQAM (C-SQAM). It is noted that C-SQAM can be defined for any positive integer M, unlike SQAM.

2.2 Bits-to-Symbol Mapping

For binary data transmission, a unique bit string should be assigned to a symbol in a constellation. Since Gray mapping does not apply to the proposed constellation, we should consider other bits-to-symbol mapping methods.

In the sense of minimizing the Gray coding penalty G_p, the average of the number of bit differences between a symbol and its adjacent neighbors, the optimum bit mapping of C-SQAM surely exists. However, the finding of the optimum mapping requires a full search of $M!$ candidates, which is not feasible for a large M.

Thus, we propose a more practical mapping method

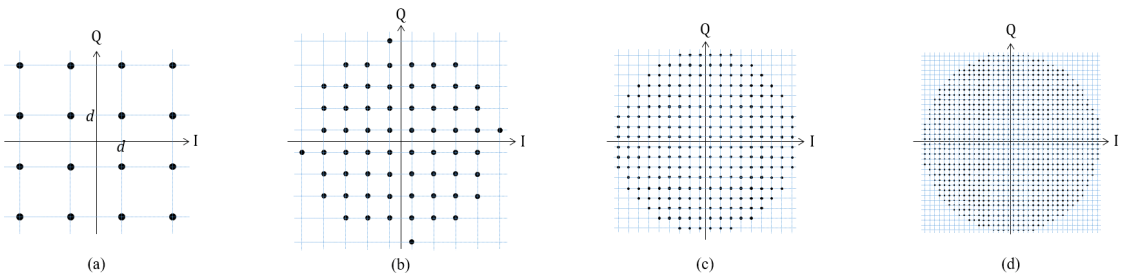

Fig. 2. C-SQAM constellation: (a) 16-ary, (b) 64-ary, (c) 256-ary, (d) 1024-ary

that keeps a low value of G_p. The following procedure is applied for the bit mappings of symbols located in the first quadrant of C-SQAM:

[Step 1] For the C-SQAM symbol located at the same position as the SQAM symbol, allocate the identical bit string.

[Step 2] For the remaining symbols, allocate as many symbols as possible while maintaining the Gray coding penalty at one.

[Step 3] For the symbols that are still unallocated, find the best bit mapping through a brute-force search.

For example, Fig. 3 shows the proposed bit mappings for the first quadrant symbols of the 256-ary C-SQAM. The 58 black-colored symbols are placed at the same position as SQAM, and they inherit the bit strings of SQAM by step 1. Among the six remaining symbols, the five red-colored symbols are allocated by step 2. Note that the Gray coding penalty is still 1 for the 63 bit-mapped symbols until now. Since only one symbol is left, the remaining bit string, 10111011, is naturally assigned to the blue-colored symbol.

Similarly, 233, 19, and 4 symbols out of 256 symbols in the first quadrant of the 1024-ary C-SQAM are allocated by step 1, step 2, and step 3, respectively, which means that only 4! searches complete the bit mappings of the first quadrant.

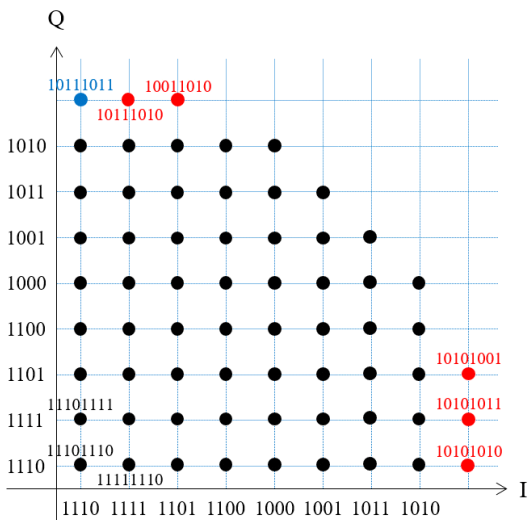

Fig. 3. Bits-to-symbol mapping of 256-ary C-SQAM (first quadrant)

Further, once the bit mappings of the first quadrant are completed, the other quadrants apply the same method used in the first quadrant to map bit strings to symbols located in their area.

Ⅲ. Performance Analysis

3.1 Error Probabilities

The probability of symbol error (SER) for an M-ary signal set can be approximated in additive white Gaussian noise (AWGN) channel as

$$P_s \approx \eta \cdot Q\left(\sqrt{\frac{2d^2}{N_0}}\right) \tag{3}$$

where η is the average number of the nearest neighbors for a symbol in a constellation, Q(·) is the Gaussian Q-function, and $N_0/2$ is the double-sided noise power spectral density. Further, the probability of bit error (BER) is approximated as

$$P_b \approx \frac{G_p}{\log_2 M} P_s \tag{4}$$

Because most symbol errors are caused by incorrectly detecting the transmitted symbol for one of its adjacent symbols, G_p bit errors occur among $\log_2 M$ bits allocated to a symbol.

For the M-ary C-SQAM, the values of η, the average symbol energy normalized by d^2, and G_p calculated from the proposed bit mapping method are summarized in Table 1. For comparison, the corresponding values for SQAM are also included, i.e., $\eta = 4\left(1 - 1/\sqrt{M}\right)$, $E_s/d^2 = 2(M-1)/3$, and G_p is always one. Note that η and the average symbol energy of C-SQAM are smaller than those of SQAM owing to a circular boundary. Although G_p of 64-ary

Table 1. Parameters depending on constellation

	SQAM			C-SQAM		
M	η	E_s/d^2	G_p	η	E_s/d^2	G_p
16	3	10	1	3	10	1
64	3.5	42	1	3.375	41	1
256	3.75	170	1	3.7188	162.75	1.0182
1024	3.875	682	1	3.8594	651.78	1.0244

C-SQAM is still one, for a larger M, G_p of C-SQAM exceeds one slightly due to the incomplete Gray mapping. Since the symbol energy is the most dominant parameter in SER and BER, C-SQAM is expected to outperform SQAM.

3.2 Asymptotic Power Gain

To derive the asymptotic gain of C-SQAM over SQAM, we consider a new normalized symbol energy, $(E_s/d^2)/M$. Then, the limit of this normalized energy for SQAM is given as

$$\lim_{M\to\infty}\left(\frac{E_s/d^2}{M}\right)_S = \lim_{M\to\infty}\frac{2}{3}\left(1-\frac{1}{M}\right)=\frac{2}{3} \tag{5}$$

Since the closed-form expression for E_s of the M -ary C-SQAM does not exist due to the lack of regularity, a different method is introduced for further analysis. Let us consider that a constellation is formed on a region $\mathcal{R}$ and signal points are uniformly distributed in the area of $\mathcal{R}$. If $\mathcal{R}$ is sufficiently large, the average symbol energy E_s can be approximated by the second moment of the region, $\mathcal{E}(\mathcal{R})$,

$$E_s \approx \mathcal{E}(\mathcal{R}) = \frac{1}{S(\mathcal{R})}\int_{\mathcal{R}} \|s_i\|^2 \, dx \tag{6}$$

where $S(\mathcal{R})$ represents the area of the region $\mathcal{R}$. Thus, for a circle-shaped constellation centered at the origin with radius r, $\mathcal{E}(\mathcal{R})$ is calculated as

$$\mathcal{E}(\mathcal{R}) = \frac{\pi r^4/2}{\pi r^2} = \frac{r^2}{2} \tag{7}$$

Further, the total number of signal points placed on the region $\mathcal{R}$ converges to

$$M = \frac{\pi r^2}{(2d)^2} \tag{8}$$

because each signal point occupies an area of $(2d)^2$ in the constellation based on a square lattice. By substituting (8) into (7), we obtain

$$\mathcal{E}(\mathcal{R}) = \frac{1}{2}\frac{(2d)^2}{\pi}M \tag{9}$$

Therefore, the limit of the normalized energy for C-SQAM becomes

$$\lim_{M\to\infty}\left(\frac{E_s/d^2}{M}\right)_C = \frac{\mathcal{E}(\mathcal{R})/d^2}{M} = \frac{2}{\pi} \tag{10}$$

The exact values of $(E_s/d^2)/M$ of C-SQAM with respect to M, $((E_s/d^2)/M)_C$, are calculated and listed in Table 2. It is observed that they converge quickly to the theoretical value, $2/\pi$ ($\approx$0.6366).

From (5) and (10), the asymptotic power gain of C-SQAM over SQAM is given as

$$\mathrm{PG}_{asymp} \lim_{M\to\infty}\frac{\left(\frac{E_s/d^2}{M}\right)_S}{\left(\frac{E_s/d^2}{M}\right)_C} = \frac{2/3}{2/\pi} = \frac{\pi}{3} \tag{11}$$

which means that the asymptotic gain in dB is equal to 0.2003dB(= 10 log(π/3)). It is worth noting in Table 2 that the power gain approaches the asymptotic value of 0.2003dB as M increases.

Table 2. Normalized energy and power gain

M	$\left(\frac{E_s/d^2}{M}\right)_S$	$\left(\frac{E_s/d^2}{M}\right)_C$	PG [dB]
16	0.625	0.625	-
64	0.6563	0.6406	0.1047
256	0.6641	0.6357	0.1893
1024	0.6660	0.6365	0.1968

3.3 PAPR

The PAPR, defined as the ratio of peak power to average power, is a crucial factor for evaluating a constellation because it is closely related to the design of a power amplifier. The PAPR of C-SQAM ($\mathrm{PAPR_C}$) is calculated and listed in Table 3 along with the PAPR of SQAM ($\mathrm{PAPR_S}$). The results show that C-SQAM has a significantly lower PAPR than SQAM, and the PAPR gain increases with the increase of M. This is because the boundary of C-SQAM gradually approaches a circle as M increases.

An exact analysis of the asymptotic PAPR can be performed as follows. For a circle-shaped constellation centered at the origin with radius r, $\mathcal{E}(\mathcal{R})$ is equal to $r^2/2$ in (7). Since the maximum symbol

Table 3. PAPR gain

M	$PAPR_S$	$PAPR_C$	PAPR gain [dB]
16	1.8	1.8	-
64	2.3333	2	0.6695
256	2.6471	1.9293	1.3735
1024	2.8182	2.0037	1.4813

energy $E_{max} = r^2$ at the circumference of the circle, the asymptotic PAPR of C-SQAM becomes

$$\mathrm{PAPR}_{\mathrm{C},asymp} = \frac{E_{max}}{\mathcal{E}(\mathcal{R})} = 2 \tag{12}$$

Similarly, for a square-shaped constellation centered at the origin with a side length of $2r$, $\mathcal{E}(\mathcal{R})$ is calculated from (6) as

$$\mathcal{E}(\mathcal{R}) = \frac{8r^4/3}{4r^2} = \frac{2r^2}{3} \tag{13}$$

Since $E_{max} = 2r^2$ at the edge of the square envelope, $(\pm r, \pm r)$, the asymptotic PAPR of SQAM becomes

$$\mathrm{PAPR}_{\mathrm{S},asymp} = \frac{2r^2}{2r^2/3} = 3 \tag{14}$$

From (12) and (14), we infer that $PAPR_S$ and $PAPR_C$ in Table 3 will converge to 3 and 2, respectively, as M increases. This suggests that a 33% reduction in PAPR, i.e., the PAPR gain of 1.7609dB(= 10 log(3/2), could be achieved using a constellation with a circular boundary instead of a square boundary. In addition, it is noteworthy that a lattice type does not affect the analysis of $PAPR_{C,asymp}$ and $PAPR_{S,asymp.}$

Ⅳ. Numerical Results

This section evaluates the performance of the proposed C-SQAM in the AWGN channel. Fig. 4 is the plot of SER and BER as a function of E_s/N_0 for the 1024-ary signal sets. From the results, it is observed that the power gains provided by C-SQAM over SQAM are 0.1982 dB at the target SER of 10^{-6} and 0.1888 dB at the target BER of 10^{-6}. It is also noted that there is a coincidence between analytical and simulation results at a wide range of E_s/N_0.

Fig. 5 shows the power gains of C-SQAM over SQAM against target error rates, which are calculated from (3) and (4). According to the results, the gain in SER and the gain in BER get closer with the decrease in error rate. The two gains converge to 0.1968 dB for M= 1024 and 0.1893dB for M= 256 as expected in Table 2. In error-prone regions, the SER gain is slightly higher than the limiting value because η of C-SQAM is smaller than η of SQAM, whereas the BER gain is lower than the limit because G_p of C-SQAM is larger than G_p of SQAM, as shown in Table 1.

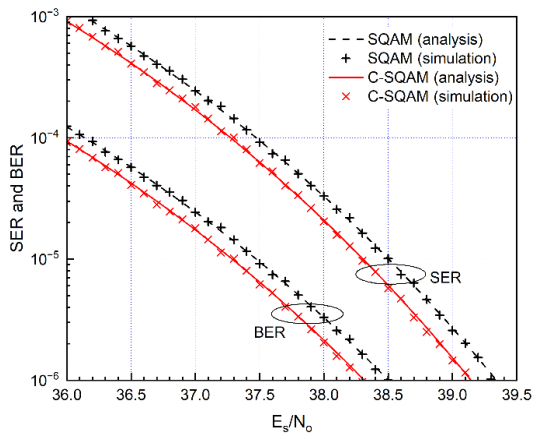

Fig. 4. Error rates of C-SQAM: M=1024

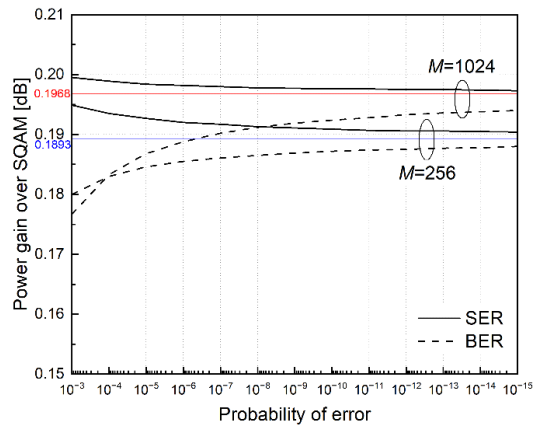

Fig. 5. Power gains of C-SQAM over SQAM

Ⅴ. Conclusions

In this study, we investigated a square-lattice quadrature amplitude modulation with a circular boundary and proposed methods for symbol selection and bits-to-symbol mapping. Performance analysis established that the power gain of C-SQAM over SQAM approaches 0.2003 dB and the PAPR of C-SQAM is asymptotically reduced to two-thirds of the PAPR of SQAM. We also confirmed that the power gains of C-SQAM in SER and BER converge fast to theoretical values.

References

[1] C. Cahn, "Combined digital phase and amplitude modulation communication systems," *IEEE Trans. Commun.*, vol. 8, no. 3, pp. 150-155, Sep. 1960. (https://doi.org/10.1109/TCOM.1960.1097623)

[2] J. Hancock and R. Lucky, "Performance of combined amplitude and phase-modulated communication systems," *IEEE Trans. Commun.*, vol. 8, no. 4, pp. 232-237, 1960. (https://doi.org/10.1109/TCOM.1960.1097638)

[3] C. Compopiano and B. Glazer, "A coherent digital amplitude and phase modulation scheme," *IEEE Trans. Commun.*, vol. 10, no. 1, pp. 90-95, 1962. (https://doi.org/10.1109/TCOM.1962.1088634)

[4] G. Foschini, R. Gitlin, and S. Weinstein, "Optimization of two-dimensional signal constellations in the presence of Gaussian noise," *IEEE Trans. Commun.*, vol. 22, no. 1, pp. 28-38, 1974. (https://doi.org/10.1109/TCOM.1974.1092061)

[5] S.-J. Park, "Triangular quadrature amplitude modulation," *IEEE Commun. Lett.*, vol. 11, no. 4, pp. 292-294, 2007. (https://doi.org/10.1109/LCOM.2007.348278)

[6] G. Forney, R. Gallager, G. Lang, F. Longstaff, and S. Qureshi, "Efficient modulation for band-limited channels," *IEEE J. Sel. Areas Commun.*, vol. 2, no. 5, pp. 632-647, 1984. (https://doi.org/10.1109/JSAC.1984.1146101)

[7] L. Hanzo, W. Webb, and T. Keller, *Single and Multi-Carrier Quadrature Amplitude Modulation*, John Wiley & Sons, 2000.

[8] S. Son and H. Park, "Design of 32-non-square QAM constellation and its channel coding," in *Proc. KICS Fall Conf. 2021*, pp. 565-566, 2021.

Minuk Seong

Feb. 2022 : B.S. degree, Gangneung-Wonju National University

Mar. 2022~Current : M.S. student, Gangneung-Wonju National University

<Research Interests> Digital communications, wireless communications, AI technology

[ORCID:0009-0001-8629-1851]

Sung-Joon Park

Feb. 1996 : B.S. degree, Yonsei University

Feb. 1998 : M.S. degree, KAIST

Feb. 2004 : Ph.D. degree, KAIST

Apr. 2005~Current : Professor, Department of Electronic Engineering, Gangneung-Wonju National University

<Research Interests> Digital communications, wireless communications, AI-based communications

[ORCID:0000-0003-4222-825X]